Mucosal administration of the B subunit of *E. coli* heat-labile enterotoxin promotes the development of Foxp3-expressing regulatory T cells

DS Donaldson[1], KK Tong[1] and NA Williams[1]

Understanding the processes by which certain mucosal pathogens and their products induce regulatory T cells (Tregs) is important in determining mechanisms of pathogenicity and may point toward their use in treating immunological disorders. Accordingly, we have studied the events that follow mucosal administration of the B subunit of *E. coli* heat-labile enterotoxin (EtxB). EtxB modulates the response to co-administered antigens and can prevent autoimmune disease. Our data show that EtxB translocates across the nasal epithelium, modulating the expression of interleukin-10 (IL-10) and transforming growth factor-β_1 (TGF-β_1). The modulated microenvironment drives an increase in Forkhead box P3 (Foxp3)-positive T cells, predominantly in the $CD4^+CD25^-$ subset. Adoptive transfer experiments showed that enhanced Foxp3 expression was particularly evident in recently activated T cells by concomitant unrelated antigen challenge, and was both TGF-β_1 and IL-10 dependent. This ability to alter T-cell differentiation pathways following mucosal delivery explains how EtxB may modify mucosal immune environments and prevent unwanted pathologies.

INTRODUCTION

Since the discovery that subsets of $CD4^+$ T cells prevent autoimmune disease development,[1] immunosuppression by $CD4^+$ regulatory T cells (Tregs) has been identified as a critical mechanism controlling self-reactivity. A number of Treg subsets have been described, including thymically derived "natural" Treg[2] and a variety of peripherally induced subsets.[3,4] Although originally characterized by expression of CD25,[1] natural Tregs are more specifically identified by expression of Forkhead box P3 (Foxp3).[5,6] Foxp3 is uniquely expressed by murine αβ T-cell receptor (TCR)-expressing $CD4^+$ T cells with suppressive activity,[7] and confers suppressive activity to $CD4^+CD25^-$ T cells.[6] Transforming growth factor-β_1 (TGF-β_1) induces *de novo* Foxp3 expression in human[8,9] and murine $CD4^+CD25^-$ T cells *in vitro*.[10] Tregs can be generated during infection with many pathogens, potentially limiting immunopathology.[11] The mechanisms by which Treg responses are stimulated by pathogens are not clear, and harnessing these, particularly at mucosal sites, is an attractive treatment option for a variety of immunopathologies.

Treatment with pathogens has inherent dangers, and the identification of specific pathogen-derived factors responsible for inducing mucosal Treg responses is advantageous. One such molecule that has this effect when applied mucosally is the *Escherichia coli* heat-labile enterotoxin B subunit (EtxB), a non-toxic derivative of the *E. coli* heat-labile enterotoxin (Etx), the cause of travelers' diarrhea and a close relative of cholera toxin (Ctx). In the non-obese diabetic mouse model of type 1 diabetes (T1D), intranasal (i.n.) administration of EtxB alone prevented diabetes development.[12] Similarly, intragastric or i.n. administration of EtxB was sufficient to prevent collagen-induced arthritis (CIA) development.[13] EtxB-induced protection was not associated with a T_H2 shift, determined by type II collagen (CII)-specific T-cell cytokine production and IgG isotype profiles. Furthermore, protection from CIA and T1D development was transferable with splenic $CD4^+$ T cells, suggesting modulation of Tregs.

Etx is a heterooligomeric complex composed of an enzymatic A subunit and five identical B subunits.[14] The B subunit mediates cellular entry via binding to G_{M1} ganglioside, which is ubiquitously expressed by all somatic cells, whereas the A subunit is responsible for toxicity.[15,16] Recombinant EtxB retains many of the properties of the Etx and is a potent immunomodulator in its own right, with a variety of effects on cells *in vitro*, including

[1]Cellular and Molecular Medicine, School of Medical Sciences, University of Bristol, Bristol, UK. Correspondence: NA Williams (neil.a.williams@bristol.ac.uk)

Received 26 October 2009; accepted 1 September 2010; published online 13 October 2010. doi:10.1038/mi.2010.65

polyclonal B-cell activation,[17] induction of $CD8^+$ T-cell apoptosis,[18] inhibition of $CD4^+$ T cell proliferation,[19] and modulation of monocyte function.[20] These functions are dependent on receptor binding as EtxB(G33D), a mutant containing a single amino acid substitution that disrupts receptor binding, was unable to mediate these effects.

In order to determine the mechanism by which EtxB modulates Tregs at mucosal sites, a variety of parameters, including the distribution of EtxB following i.n. treatment, the effect of EtxB treatment on cytokine expression, and the effect of EtxB treatment on Foxp3 expression, have been investigated *in vivo*. The effect of EtxB on Foxp3 expression within antigen-specific $CD4^+$ T cells and how blocking antibodies against immunoregulatory cytokines affect the outcome of EtxB treatment was also investigated.

RESULTS

Distribution of EtxB following i.n. administration

Mucosal administration of EtxB modulates T-cell responses to unrelated antigens;[12,13] however, the site where this occurs is unknown. In initial experiments, the distribution of EtxB and the non-receptor binding mutant, EtxB(G33D), following i.n. delivery on four consecutive days was determined using immunohistochemistry. Nasal-associated lymphoid tissue (NALT), cervical lymph nodes (CLNs), and spleen were removed on days 1 and 4 following treatment, paraffin-embedded, and stained for EtxB or EtxB(G33D) using a cross-reactive polyclonal anti-cholera toxin antibody. EtxB was detected in the NALT, CLNs, and spleen after EtxB treatment (**Figure 1**). EtxB was primarily found in the epithelial layer of the NALT; however, discrete cells were also observed within the NALT. $EtxB^+$ cells were scattered throughout the CLNs, and were mainly located adjacent to white pulp areas of the spleen. The area of positive staining in each sample was calculated and expressed as a percentage of the total area. As would be expected, most EtxB was found in the NALT, the site closest to administration, which contained 6-fold and 40-fold more staining than in the CLNs and spleen, respectively. In the NALT (including epithelial cell layer) and CLN, levels of EtxB staining were maximal on day 1 and remained above background levels on day 4. In contrast, the level of EtxB staining in the spleen on day 1 returned to background levels by day 4. No EtxB(G33D) was found in any of the tissues tested, highlighting the critical role of receptor binding in the uptake and trafficking process.

In order to determine which cells bound EtxB, mice were treated i.n. with Alexa 647 (Invitrogen, Paisley, UK)-labeled EtxB on four consecutive days, and the phenotypes of Alexa 647-labeled $EtxB^+$ cells in the CLN and spleen analyzed by flow cytometry. Unlabeled EtxB-treated mice were used as controls. A small population of Alexa 647^+ cells were detectable in the CLNs and spleen (**Figure 2a**). Very few Alexa 647^+ cells were observed within the $CD4^+$ and $B220^+$ cell populations of

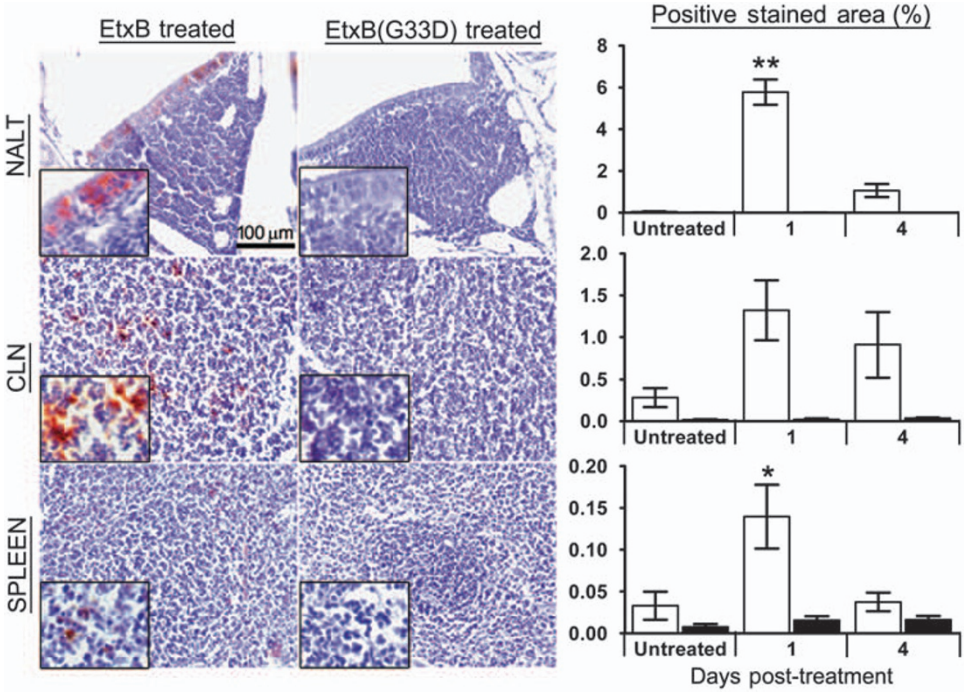

Figure 1 Distribution of *Escherichia coli* heat-labile enterotoxin B subunit (EtxB) and EtxB(G33D) following intranasal (i.n.) administration. Mice were treated with EtxB or EtxB (G33D) on four consecutive days. On days 1 and 4 post-treatment, nasal-associated lymphoid tissue (NALT), cervical lymph nodes (CLNs), and spleen were removed and embedded in paraffin wax. Sections were then stained for EtxB/EtxB(G33D) (shown as brown staining) and counterstained with hematoxylin (blue staining). Tissue sections shown are representative of day 1 post-treatment. The positive stained area in each section from EtxB-treated (white bars) or EtxB(G33D)-treated (black bars) mice was calculated by measuring the stained area (including the NALT epithelium) and expressing this as a percentage of the total area ($n=3$). Untreated mice were used as controls. Significant differences with the untreated control were determined using a one-way analysis of variance (ANOVA) with Tukey's *post hoc* test. Error bars represent s.e.m., $^*P<0.05$, $^{**}P<0.01$.

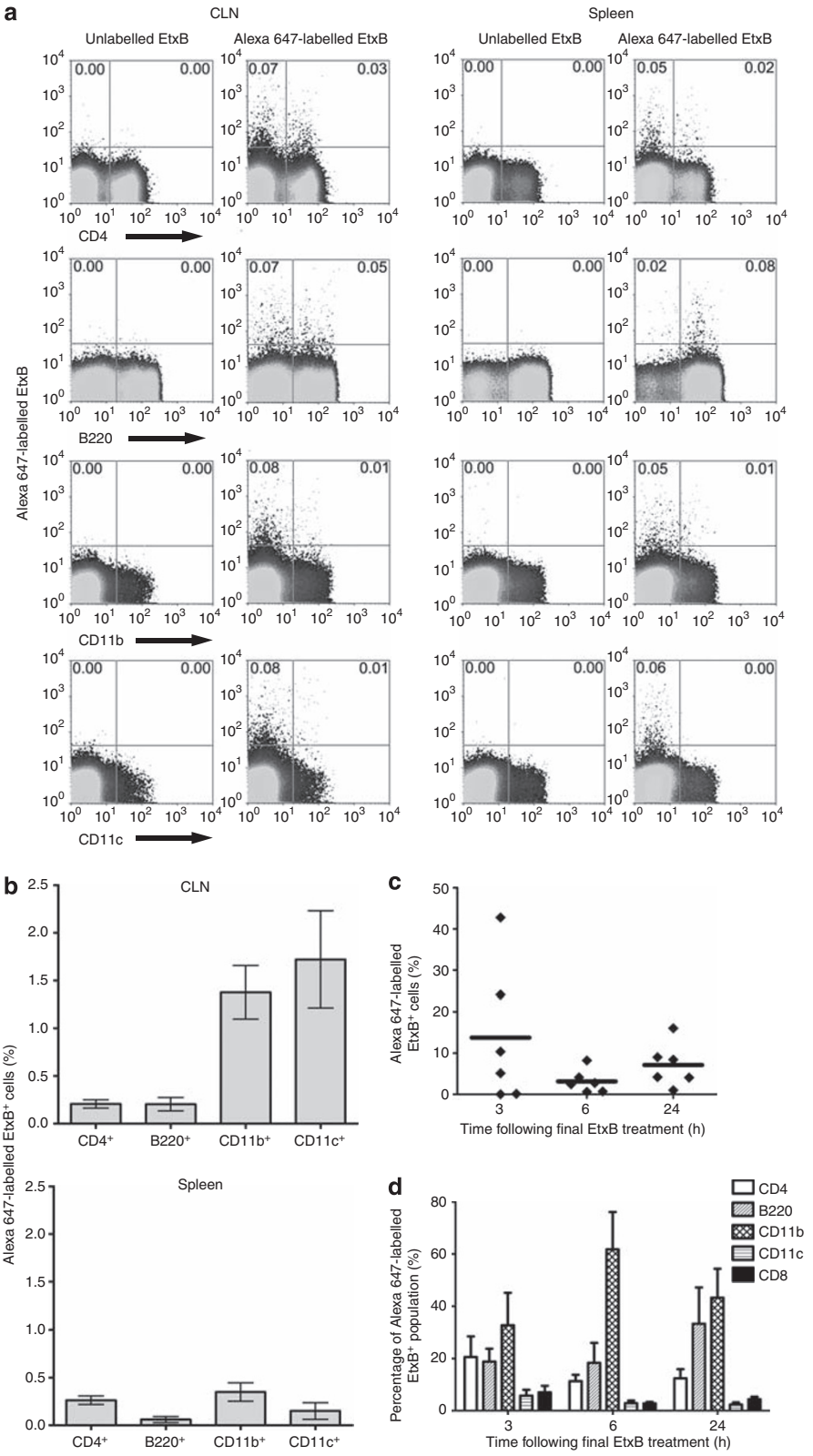

Figure 2 Phenotype of *Escherichia coli* heat-labile enterotoxin B subunit (EtxB)-positive cells in lymphoid tissues and peripheral blood. Mice were treated with Alexa 647-labeled EtxB on four consecutive days. On day 1 post-treatment, cervical lymph nodes (CLNs) and spleen were removed and enzymatically digested. The resultant cell suspensions were stained with a panel of antibodies specific for lineage markers and analyzed by flow cytometry. (**a**) Representative plots of Alexa 647-labeled EtxB$^+$ and lineage marker$^+$ cells from the CLNs and spleen of mice treated with labeled or unlabeled EtxB. (**b**) The frequency of Alexa 647-labeled EtxB$^+$ cells within each cell subset was then determined (n=3). Peripheral blood was also removed at various time points following Alexa 647-labeled EtxB treatment and the peripheral blood mononuclear cells (PBMCs) isolated, and analyzed by flow cytometry for the (**c**) presence of Alexa 647-labeled EtxB$^+$ cells (n=6) and (**d**) stained with a panel of antibodies specific for lineage markers (n=6). Error bars represent s.e.m.

the CLNs (**Figure 2b**), whereas 1.4±0.3% of the CD11b$^+$ and 1.7±0.5% of the CD11c$^+$ cell populations were Alexa 647$^+$. The spleen contained lower proportions of Alexa 647$^+$ cells, with the highest proportions in CD11b$^+$ and CD4$^+$ cells; however, these were still lower than in the CLNs.

The presence of EtxB in non-mucosal sites could reflect transport of free EtxB or the migration of cells that acquired it at the delivery site. Free EtxB was undetectable in serum using a highly sensitive enzyme-linked immunosorbent assay (data not shown). Therefore, the presence of EtxB on peripheral blood mononuclear cells was investigated. Following treatment with labeled EtxB, Alexa 647$^+$ cells were observed in the blood at all time points studied (**Figure 2c**), with the predominant population being CD11b$^+$ (**Figure 2d**).

The effect of EtxB on immunoregulatory cytokine expression

Both interleukin-10 (IL-10) and TGF-β_1 have roles in modulating the number of Tregs.[10,21,22] As EtxB was found in the NALT, CLNs, and spleen, expression of IL-10 and TGF-β_1 mRNAs in these lymphoid organs was investigated following treatment. mRNAs were isolated from pooled NALT, CLNs, and spleens of EtxB-treated mice on days 1 and 6 following treatment, and the relative expression levels of IL-10 and TGF-β_1 mRNAs determined by PCR (**Figure 3a** and **b**). EtxB treatment increased the level of IL-10 mRNA in the NALT, CLNs, and spleen, and induced a transient increase in TGF-β_1 mRNA in the same tissues. Densitometric analysis of the relative expression levels revealed that the increase in IL-10 mRNA was significant on day 1 post-treatment in all three organs tested, and that the increase in TGF-β_1 mRNA was significant on days 1 and 6 in the NALT and day 1 in the CLNs (**Figure 3b**). The mean of two independent samples also suggested that TGF-β_1 mRNA was also increased in spleen.

Confirmation of the ability of EtxB to stimulate regulatory cytokine production came from studies of NALT, CLN, and spleen tissue sections from EtxB- and EtxB(G33D)-treated mice. EtxB treatment clearly upregulated IL-10 and TGF-β_1 expression in the NALT, particularly in the epithelium (**Figure 4a** and **b**). An increase was also noted in the CLNs and spleen. Image analysis revealed that the NALT had much higher positive stained area than the CLNs (3-fold and 12-fold higher for IL-10 and TGF-β_1, respectively) or spleen (6-fold and 40-fold higher for IL-10 and TGF-β_1, respectively) because of its proximity to the site of administration. In the NALT and the overlying epithelium, this increase in IL-10 and TGF-β_1 was significant on day 1 post-treatment. Unlike in the NALT, IL-10 expression in the CLNs and spleen increased on day 1 and continued to increase by day 4, at which point it reached significance. TGF-β_1 expression was also increased in the CLNs on days 1 and 4, whereas in the spleen, a significant increase was only observed on day 1, paralleling expression in the NALT. EtxB(G33D) did not induce an increase in IL-10 or TGF-β_1 expression in any tissue tested. The presence of regulatory cytokines *per se* does not indicate that the environment is one that would stimulate Treg cell induction, and thus the expression of interferon-γ was also investigated by immunohistochemistry. No concomitant increase in interferon-γ was observed after EtxB treatment (**Supplementary Figure S1** online).

In order to identify which cell types expressed IL-10 and TGF-β_1 following EtxB treatment, subsets of cells from the CLNs of untreated and EtxB-treated mice were purified using magnetic-activated cell sorting prior to mRNA isolation. No increase in IL-10 or TGF-β_1 mRNA expression was observed in CD4$^+$ or B220$^+$ cell populations of the CLNs; however, a clear increase in IL-10 and TGF-β_1 mRNA expression was observed within the CD11b$^+$ cell population (**Figure 5a**). Densitometric analysis confirmed that the increase was significant for both cytokines (**Figure 5b**).

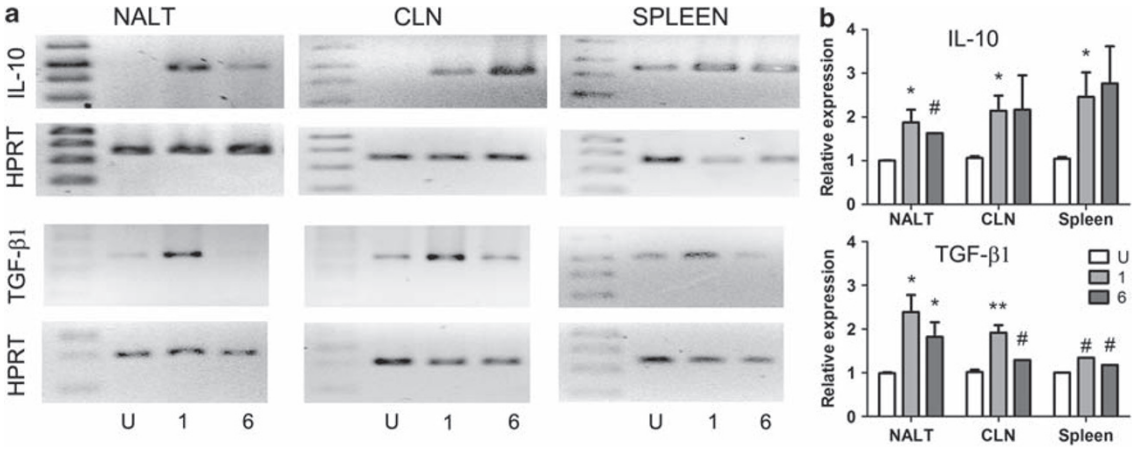

Figure 3 The effect of intranasal (i.n.) *Escherichia coli* heat-labile enterotoxin B subunit (EtxB) treatment on interleukin-10 (IL-10) and transforming growth factor-β_1 (TGF-β_1) mRNA expression in local and distant lymphoid organs. Mice were treated with EtxB on four consecutive days. mRNA was extracted from pooled nasal-associated lymphoid tissue (NALT; 10 mice), cervical lymph nodes (CLNs; 4 mice), and spleen (3 mice) removed on days 1 and 6 post-treatment. The expression of IL-10 and TGF-β_1 mRNA was analyzed by reverse transcriptase-PCR (RT-PCR), with expression of HPRT mRNA as a control. Untreated mice (U) were included for comparison. (**a**) Representative PCR gel images of IL-10 and TGF-β1 mRNA expression. (**b**) PCR gel images were subjected to densitometry analysis and the relative expression levels calculated by comparison with HPRT expression (n>3 for all experiments except those marked with # indicating the mean of two independent experiments). Significant differences with the untreated control were determined using Student's *t-test*. Error bars represent s.e.m., *P<0.05, **P<0.01.

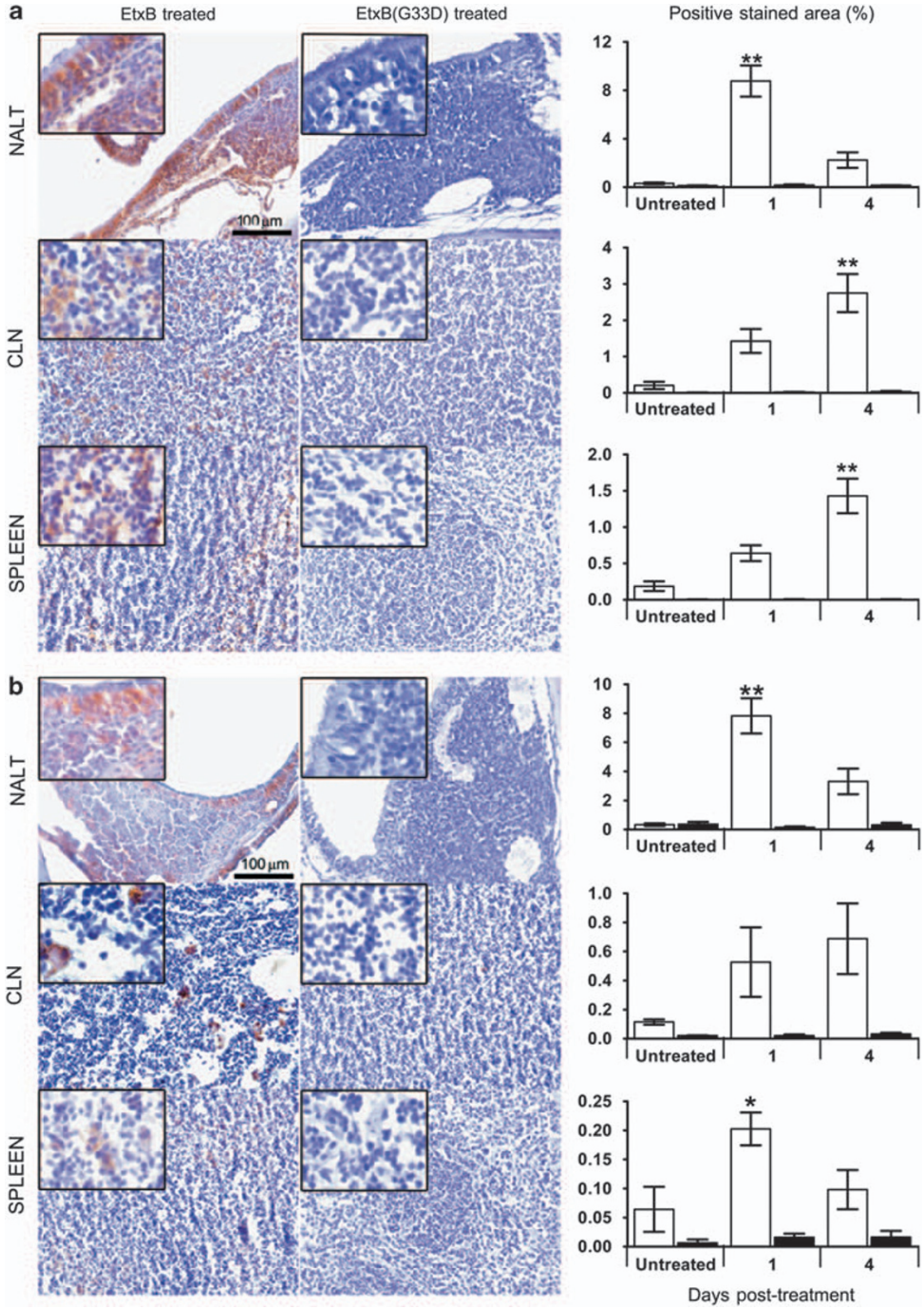

Figure 4 The effect of intranasal (i.n.) *Escherichia coli* heat-labile enterotoxin B subunit (EtxB) treatment on interleukin-10 (IL-10) and transforming growth factor-β_1 (TGF-β_1) protein expression in local and distant lymphoid organs. Nasal-associated lymphoid tissue (NALT), cervical lymph nodes (CLNs), and spleen were removed from EtxB and EtxB (G33D)-treated mice on days 1 and 4 post-treatment and embedded in paraffin wax. Sections of each tissue were stained for (**a**) IL-10 or (**b**) TGF-β_1 (brown staining) and counterstained with hematoxylin (blue staining). Tissue sections shown are representative of day 1 post-treatment. The positive stained area in each section was calculated by measuring the stained area (including the NALT epithelium) and expressing this as a percentage of the total area ($n=3$). Untreated mice were used as controls. Significant differences with the untreated control were determined using a one-way analysis of variance (ANOVA) with Tukey's *post hoc* test. Error bars represent s.e.m., $^*P<0.05$, $^{**}P<0.01$.

EtxB treatment creates a regulatory environment associated with Treg cell induction

In order to test directly whether EtxB administration was associated with increased numbers of Treg cells, a number of putative Treg markers were assessed. Initial flow cytometric studies failed to identify a difference in the proportion of $CD4^+$ T cells expressing CD25 or glucocorticoid-induced TNFR-related protein following EtxB treatment (data not shown). As neither of these fully encompasses the whole Treg population, expression of Foxp3 mRNA was also investigated in NALT, CLNs, and spleen from EtxB-treated and untreated mice (**Figure 6a**). Densitometric analysis revealed

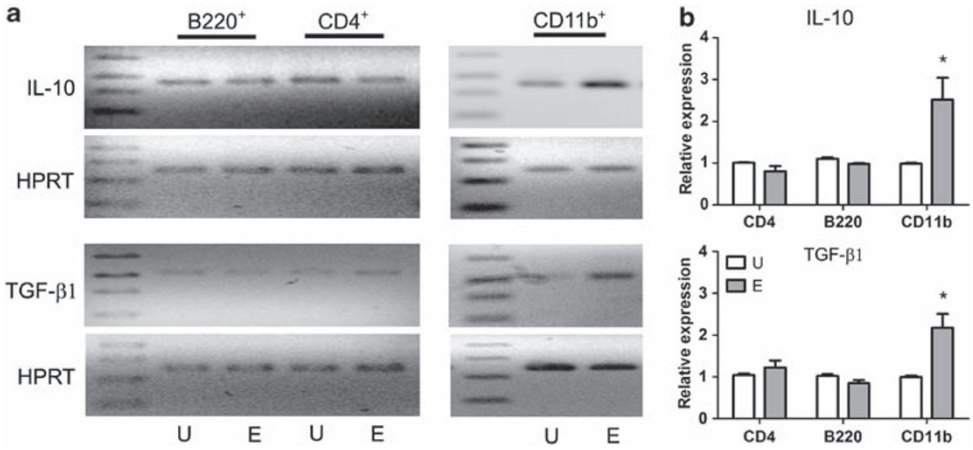

Figure 5 Expression of interleukin-10 (IL-10) and transforming growth factor-β_1 (TGF-β_1) in purified subsets from the cervical lymph nodes (CLNs) of *Escherichia coli* heat-labile enterotoxin B subunit (EtxB)-treated mice. Mice were treated with EtxB on four consecutive days. Pooled CLNs from four mice were removed on day 1 post-treatment and $CD4^+$, $B220^+$, and $CD11b^+$ cell subsets purified by magnetic-activated cell sorting (MACS). mRNA was extracted from each subset and the expression of IL-10 and TGF-β_1 mRNA was analyzed by reverse transcriptase-PCR (RT-PCR), with expression of HPRT mRNA as a control (E). Untreated mice (U) were included for comparison. (**a**) Representative PCR gel images of IL-10 and TGF-β1 mRNA expression. (**b**) PCR gels were subjected to densitometry analysis and the relative expression levels calculated by comparison with HPRT expression (B220 and CD4, $n=3$; CD11b, $n=4$). Significant differences with the untreated control were determined using Student's *t-test*. Error bars represent s.e.m., $^*P<0.05$.

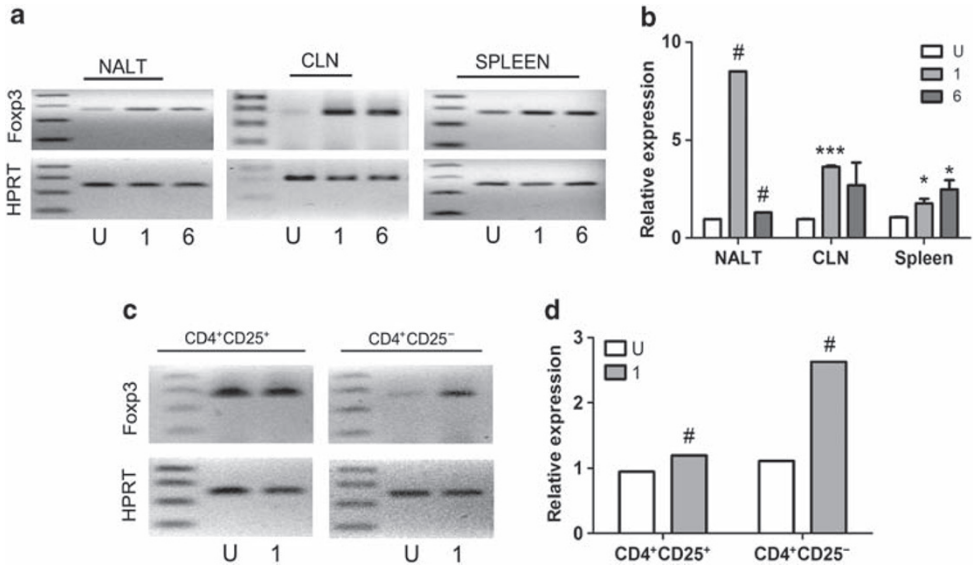

Figure 6 The effect of intranasal (i.n.) *Escherichia coli* heat-labile enterotoxin B subunit (EtxB) treatment on Forkhead box P3 (Foxp3) mRNA expression in local and distant lymphoid organs. (**a**) Mice were treated with EtxB for four consecutive days. mRNA was extracted from pooled nasal-associated lymphoid tissue (NALT; 10 mice), cervical lymph nodes (CLNs; 4 mice), and spleen (3 mice) removed on days 1 and 6 post-treatment. Expression of Foxp3 mRNA was analyzed by reverse transcriptase-PCR (RT-PCR), with expression of HPRT mRNA as a control. Untreated mice (U) were included for comparison. Representative results are shown in **a**. (**b**) PCR gel images were subjected to densitometry analysis and the relative expression levels calculated by comparison with HPRT expression ($n>3$ for all experiments except those marked with # indicating the mean of two independent experiments). (**c**) Foxp3 mRNA expression was also analyzed in fluorescence-activated cell sorting (FACS)-sorted splenic $CD4^+CD25^+$ and $CD4^+CD25^-$ T cells. (**d**) The mean of two independent experiments. Significant differences with the untreated control were determined using Student's *t-test*. Error bars represent s.e.m., $^*P<0.05$, $^{***}P<0.001$.

that EtxB treatment induced a significant increase in Foxp3 mRNA expression in the CLNs and spleen on day one post-treatment (**Figure 6b**). The mean of two independent samples indicated that an increase was also observed within NALT. A significant increase was also observed in the spleen up to 25 days post-treatment (**Supplementary Figure S2** online). Foxp3 mRNA expression was then investigated in FACS (fluorescence-activated cell sorting)-sorted splenic $CD4^+CD25^+$ and $CD4^+CD25^-$ populations following EtxB treatment (**Figure 6c**). Densitometric analysis of two independent samples showed no difference in Foxp3 mRNA expression in the $CD4^+CD25^+$ T-cell population, whereas an increase was observed in the $CD4^+CD25^-$ T-cell

population, suggesting that this increase was responsible for the increase seen in the whole CD4$^+$ T-cell population.

Increased expression of Foxp3 mRNA could result from increased CD4$^+$Foxp3$^+$ T cells or increased expression of Foxp3 within Foxp3$^+$ cells. In order to clarify this, the proportion of Foxp3$^+$ cells in the CLNs and spleen following phosphate-buffered saline (PBS) or EtxB treatment was determined by flow cytometry (**Figure 7a**). EtxB treatment induced a slight increase in the proportion of Foxp3-expressing CD4$^+$ T cells in both the CLNs and spleen (**Figure 7b**), which, although subtle, was highly reproducible. As was found with Foxp3 mRNA, the increased proportion of Foxp3-expressing CD4$^+$ T cells was mainly located in the CD25$^-$ fraction, where significant increases were observed in both tissues.

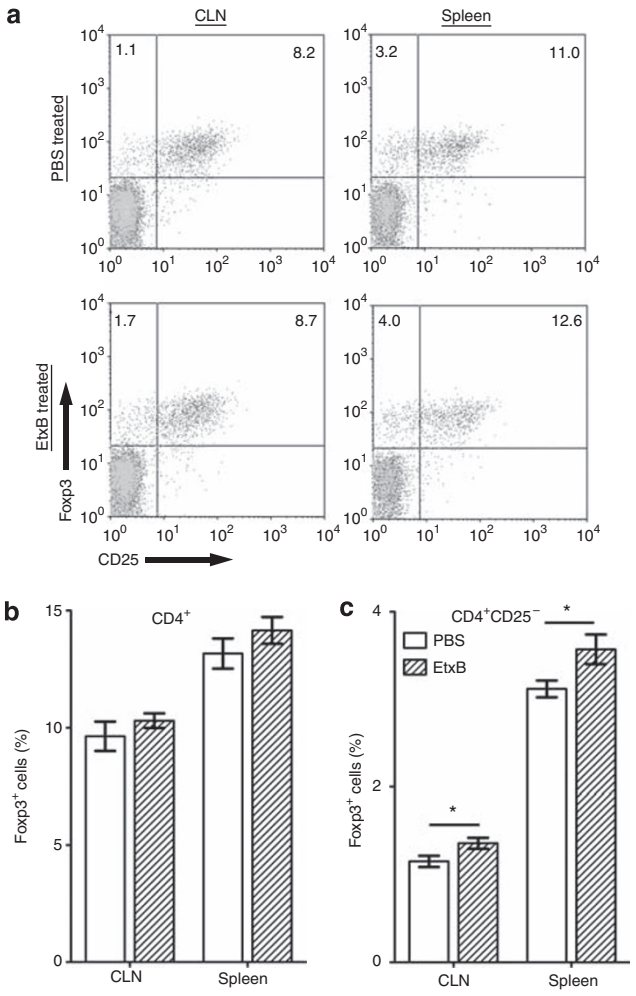

Figure 7 The effect of intranasal (i.n.) *Escherichia coli* heat-labile enterotoxin B subunit (EtxB) treatment on the proportion of Forkhead box P3 (Foxp3)-expressing CD4$^+$ T cells. Mice were treated with phosphate-buffered saline (PBS; white bars) or EtxB (hatched bars) on four consecutive days. On day 6 post-treatment, cervical lymph nodes (CLNs) and spleen were removed, stained for CD4, CD25, and Foxp3, and analyzed by flow cytometry. (**a**) Representative fluorescence-activated cell sorting (FACS) plots from EtxB and PBS treated mice. From this the proportion of (**b**) CD4$^+$ and (**c**) CD4$^+$CD25$^-$ T cells that express Foxp3 was determined (n=6). Results are representative of three separate experiments. Significant differences were determined using Student's *t-test*. Error bars represent s.e.m., *P<0.05.

Antigen specificity of the increase in Foxp3-expressing CD4$^+$ T cells

In inflammatory disease models modulated by EtxB, it has been given in the context of an inflammatory response to self-antigen, such as CII/complete Freund's adjuvant (CFA) challenge in CIA and on-going spontaneous islet inflammation in the non-obese diabetic mice.[12,13] In defining the mechanism of action, it was important to determine whether EtxB treatment was associated with the induction of Tregs specific for antigen to which the animal was actively responding at that time. In order to do so, ovalbumin (OVA) was administered in CFA, replicating the process of CIA induction, but in a system where antigen-specific CD4$^+$ T cells from DO11.10 mice, which express a TCR specific for OVA peptide, could be studied as a result of having adoptively transferred into the recipients. Briefly, splenic DO11.10 CD4$^+$ T cells were transferred into BALB/c mice followed by i.n. treatment with EtxB or PBS on four consecutive days and OVA/CFA challenge on day 1 post-treatment. On day 6, splenocytes were removed, stained for CD4, Foxp3, and the DO11.10 TCR (KJ1-26), and analyzed by flow cytometry. As expected, OVA/CFA challenge induced an overall increase in the proportion of the spleen cells that were KJ1.26$^+$ (data not shown). Importantly, EtxB induced a significant increase in the proportion of the endogenous CD4$^+$ T cells that express Foxp3 in both unchallenged and OVA-challenged mice (**Figure 8a**). In the OVA-specific population, no increase was observed in the absence of OVA challenge (**Figure 8b**), and the proportion of Foxp3$^+$ cells was equivalent to pre-transfer levels. However, in mice challenged with OVA/CFA and given EtxB, a significant increase in the proportion of Foxp3$^+$CD4$^+$ T cells was observed. A similar significant increase in the proportion of OVA-specific Foxp3$^+$CD4$^+$ T cells was observed in the CLNs (data not shown).

Effect of IL-10R and TGF-β blockade on the EtxB-induced increase in the proportion of Foxp3-expressing OVA-peptide-specific CD4$^+$ T cells

As EtxB induced both IL-10 and TGF-β_1 cytokines that have the capacity to modulate Treg numbers,[10,21,22] they may be involved in increasing the proportion of Foxp3$^+$CD4$^+$ T cells. In order to establish their role, the effect of blocking the IL-10 receptor (IL-10R) or TGF-β *in vivo* in the context of EtxB treatment was investigated. DO11.10 CD4$^+$ T cells were adoptively transferred into BALB/c mice prior to i.n. treatment with EtxB or PBS on four consecutive days. On the third day of treatment, 0.5 mg of anti-IL-10R or anti-TGF-β, or an equivalent concentration of control IgG, was administered intraperitoneally. On day 1 post-treatment, mice were challenged with OVA/CFA. On day 6 post-treatment, splenocytes were removed and analyzed by flow cytometry for the presence of CD4, the DO11.10 TCR, and Foxp3. EtxB treatment induced a significant increase in the proportion of Foxp3$^+$ OVA-specific CD4$^+$ T cells following normal rat (**Figure 9a**) or mouse (**Figure 9b**) IgG administration. However, following administration of anti-IL-10R (**Figure 9a**)

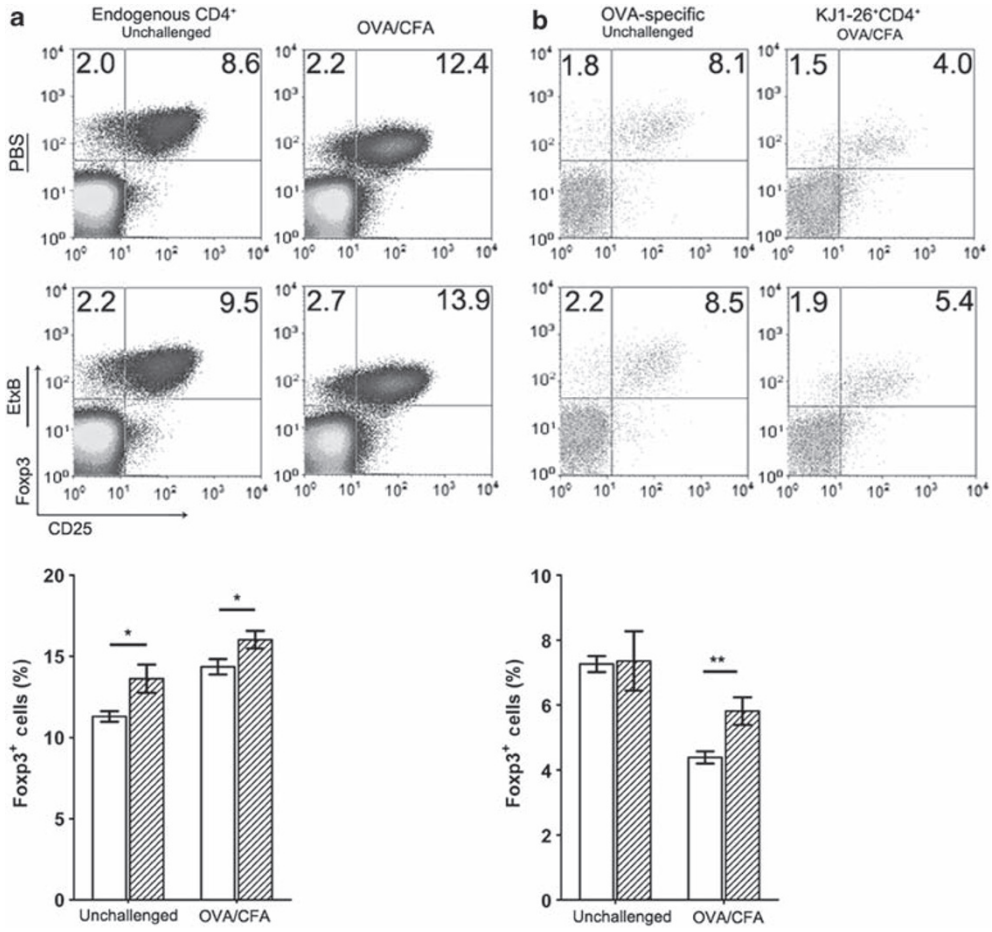

Figure 8 The effect of intranasal (i.n.) *Escherichia coli* heat-labile enterotoxin B subunit (EtxB) treatment on the proportion of Forkhead box P3 (Foxp3)-expressing ovalbumin (OVA)-specific CD4$^+$ T cells. DO11.10 CD4$^+$ T cells (KJ1-26$^+$) were adoptively transferred into BALB/c prior to i.n. treatment with phosphate-buffered saline (PBS; white bars) or EtxB (hatched bars) on four consecutive days. Following EtxB treatment, mice were either left unchallenged or challenged with OVA/complete Freund's adjuvant (CFA) on day 1 post-treatment. On day 6, the spleen was removed, stained for CD4, CD25, DO11.10 T-cell receptor (TCR; KJ1-26), and Foxp3, and analyzed by flow cytometry. From this the proportion of the (**a**) endogenous (KJ1-26$^-$) CD4$^+$ and (**b**) OVA-specific (KJ1-26$^+$) CD4$^+$ T-cell populations that express Foxp3 was calculated (n=6). Representative fluorescence-activated cell sorting (FACS) plots of individual mice are shown in the upper panel. Significant differences were determined using Student's *t-test*. Error bars represent s.e.m., *P<0.05, **P<0.01.

or anti-TGF-β (**Figure 9b**), no difference in the proportions of Foxp3$^+$ OVA-specific CD4$^+$ T cells was observed in the spleen of PBS and EtxB-treated mice. Anti-IL-10R and anti-TGF-β also blocked the increase in Foxp3 in the endogenous CD4$^+$ T-cell population (data not shown). Interestingly, both anti-IL-10R and anti-TGF-β treatment did cause a slight increase in overall numbers of KJ1-26$^+$CD4$^+$Foxp3$^+$ cells in control animals; however, this appeared to be related to antigen stimulation as it was not observed in the endogenous CD4$^+$ T-cell population (data not shown).

DISCUSSION

EtxB has an extremely high affinity for its principle receptor, ganglioside G_{M1},[23] and although it would be expected to bind epithelial cells, the fact that it enters the body and was detected in blood and lymphoid tissues was unexpected. EtxB clearly bound the nasal epithelium, conforming with a previous study showing intestinal epithelial localization following oral delivery.[24] In this study, EtxB was shown to traffic beyond the epithelial layer, being detectable as far as in the spleen. EtxB transcytoses across polarized epithelium and can be detected basolaterally,[24,25] potentially the mechanism by which it enters the body. EtxB may also have reached the lung in significant quantities, potentially serving as an additional entry point. The receptor dependency of binding and uptake of EtxB was evident from the lack of EtxB(G33D) staining and is in keeping with the failure of the mutant to modulate immune responses and protect from CIA and T1D development.[12,13]

The location of EtxB in lymphoid tissues correlated with the location of IL-10 and TGF-β_1, suggesting that their upregulation may be a direct consequence of EtxB-mediated signaling, particularly in the NALT, where all were in the epithelial layer, and temporally correlated with each other. The possibility that modulation of epithelial cytokine production has a key part in the ability of EtxB to establish an immune environment favoring Treg responses is intriguing. It is unclear whether recently activated T cells enter the NALT and become exposed to this environment; however, it remains likely that this environment would influence

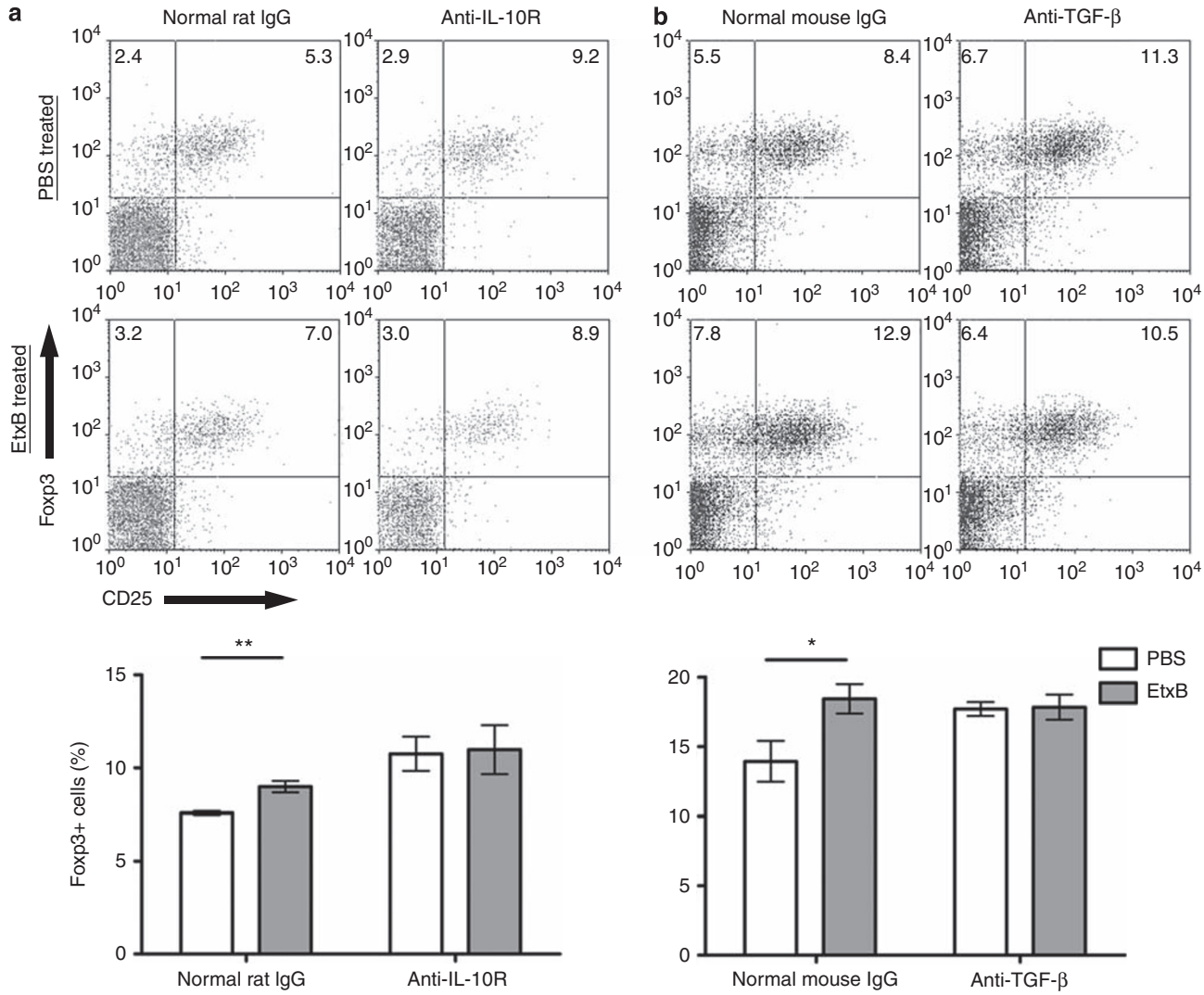

Figure 9 The effect of blocking antibodies against interleukin-10 (IL-10) and transforming growth factor-β (TGF-β) on the *Escherichia coli* heat-labile enterotoxin B subunit (EtxB)-induced increase in proportion of Forkhead box P3 (Foxp3)-expressing ovalbumin (OVA)-specific $CD4^+$ T cells. DO11.10 $CD4^+$ T cells (KJ1-26^+) were adoptively transferred in BALB/c mice prior to intranasal (i.n.) treatment with either phosphate-buffered saline (PBS; white bars) or EtxB (filled bars) on four consecutive days. On the third day of EtxB or PBS treatment, 0.5 mg of (**a**) anti-IL-10R or (**b**) anti-TGF-β was administered intraperitoneally. Control mice were given an equivalent amount of normal mouse or rat IgG. On day 1 post-treatment, mice were challenged with OVA/complete Freund's adjuvant (CFA). On day 6, the spleen was removed, stained for CD4, DO11.10 T-cell receptor (TCR; KJ1-26), and Foxp3, and analyzed by flow cytometry. From this the proportion of the OVA-peptide specific (KJ1-26^+) $CD4^+$ T-cell population that express Foxp3 was calculated (n=5). Representative fluorescence-activated cell sorting (FACS) plots of individual mice are shown in the upper panel. Results are representative of two separate experiments. Significant differences were determined using Student's *t-test*. Error bars represent s.e.m., *P<0.05, **P<0.01.

the response to antigens co-delivered with EtxB, consistent with its ability to promote mucosal antibody responses.[26]

EtxB induces IL-10 secretion from human monocytes *in vitro,*[20] and in accordance with this, increased IL-10 and TGF-β_1 were found in $CD11b^+$ cells of the CLNs. More IL-10^+ than $EtxB^+$ cells were observed, and although it is possible that degradation of EtxB limits the numbers of cells upon which staining is observed, this may suggest that a proportion of the increase results from an indirect effect of EtxB. The uptake of EtxB-induced apoptotic $CD8^+$ T cells[18] could also stimulate IL-10 and TGF-β_1 expression.[27] Although we have consistently failed to show a reduction in the proportion of $CD8^+$ or $CD4^+$ T cells in the CLNs or spleen following EtxB treatment (data not shown), it remains possible that some cell death, either locally or at low levels, could contribute to the increased IL-10 and TGF-β_1 expression.

The increased proportion of Foxp3-expressing $CD4^+$ T cells found after EtxB treatment are likely to be responsible for its ability to prevent autoimmune disease development in a manner that is transferable with $CD4^+$ T cells. The strong association between expression of Foxp3 and regulatory function in the mouse makes it highly likely that these changes are associated with the generation of enhanced regulation. Although in other systems, increases in Foxp3 expression have been shown to be transitory in nature,[28] the EtxB-induced changes are stable. Additionally, mucosal administration of CtxB-antigen conjugates that have a similar effect to that of EtxB administration also induce an

increase in Foxp3-expressing $CD4^+$ T cells,[29,30] supporting the notion that these cells are responsible for the effects of EtxB in CIA and T1D. The increase we observed was predominantly in the $CD25^-$ fraction. Our previous studies have shown that removal of either the $CD25^+$ or $CD25^-$ fraction from splenic $CD4^+$ T cells before adoptive transfer from EtxB-treated mice partially abrogated their ability to suppress the development of CIA, arguing a role for both populations. Adoptive transfer of $CD4^+CD25^-$ T cells was not as effective as the reciprocal $CD25^+$ fraction,[13] likely because of the lower frequency of $Foxp3^+$ cells. The $CD4^+CD25^+$ T-cell fraction also showed enhanced regulatory activity *in vitro* following *in vivo* EtxB treatment,[13] suggesting that this population may be the most important for protection, and the observed increase in the $CD25^-$ fraction may be a by-product of this expansion. Furthermore, it is conceivable that expression of CD25 may alter within the longer time frames used in the published adoptive transfer experiments. Ideally, one would wish to sort an EtxB-induced population; however, although increases in the Treg markers Foxp3, CD38, surface TGF-β_1, and CTLA-4 were observed after EtxB treatment (data not shown), naive mice also contain sizable populations of cells expressing these markers, making isolation problematic. The increase in the proportion of Foxp3-expressing $CD4^+$ T cells could have occurred via two mechanisms: *de novo* induction of Foxp3 expression in $CD4^+Foxp3^-$ T cells or expansion of $CD4^+Foxp3^+$ T cells. Intranasal administration of EtxB and OVA has been shown to induce the proliferation of OVA-peptide-specific $CD4^+$ T cells in the CLNs; however, the $CD4^+CD25^+$ subset was shown not to proliferate.[31] This would suggest that EtxB treatment induces *de novo* induction of Foxp3 expression in $CD4^+$ T cells, supported by the fact that the increase was predominantly in the $CD25^-$ subset.

Importantly, EtxB treatment induced an increase in the proportion of Foxp3-expressing OVA-specific $CD4^+$ T cells in the spleens of OVA/CFA-challenged animals. We hypothesize that it is this shift in the balance of Treg vs. effector T cells that biases the immune system toward regulation rather than pathogenic responses. The lower levels of $Foxp3^+$ cells in OVA/CFA-challenged mice compared with unchallenged mice probably reflects preferential expansion of effector cells under both conditions, not all of which is prevented by EtxB treatment. Blocking of IL-10R or TGF-β_1 abrogated the ability of EtxB to induce an increase in the proportion of Foxp3-expressing OVA-specific $CD4^+$ T cells. Blocking TGF-β_1 also abrogated increased $Foxp3^+$ OVA-specific $CD4^+$ T cells induced following oral administration of a CtxB-OVA conjugate.[30] A general increase in the proportion of OVA-specific $CD4^+$ T cells was observed following administration of either antibody; however, this was an antigen-driven process and was not observed in the endogenous $CD4^+$ T-cell population, implying that it may have been related to increased activation and IL-2 in the absence of regulation. Other studies using these antibodies have also observed an increase in Foxp3-expressing cells of a similar magnitude.[30] Additionally, an increase was also noted in mice treated with normal mouse IgG, the reason for which was undetermined; however, this did not affect the ability of EtxB to induce an increase in Foxp3-expressing cells. Both of these cytokines have been shown to be involved in either the expansion or induction of Tregs. TGF-β_1 induces *de novo* expression of Foxp3 in $CD4^+CD25^-$ T cells *in vitro* and *in vivo*.[10] Systemic overexpression of IL-10 increases the proportion of $CD4^+CD25^+$ T cells in a dose-dependent fashion.[22] A direct effect of IL-10 on Tregs has not been demonstrated; however, its ability to downregulate proinflammatory responses[32] and reverse the downregulation of TGF-βRII expression on activated T cells[33] may have altered the activity of TGF-β_1. Although $CD11b^+$ cells were shown to be a source of these cytokines *in vivo*, co-culture experiments using isolated $CD11b^+$ cells from EtxB-treated mice, or EtxB treatment of isolated $CD11b^+$ cells from naive animals and T cells, failed to replicate the increases in Foxp3-expressing cells observed *in vivo* (data not shown), suggesting that other aspects of the unique environment created in lymphoid tissues following EtxB treatment are also important. Further characterization of the *in vivo* effects of EtxB on this population in future may provide clues as to the processes involved.

Many insights into the mechanism by which EtxB exerts its effects *in vivo* have been gained in this study. By modulating local and systemic tissues, biasing them toward an immunoregulatory environment through the combined actions of IL-10 and TGF-β_1, EtxB effectively induced antigen-specific Tregs, previously shown to be able to protect against autoimmune disease. The question still remains as to where EtxB-induced modulation of T-cell differentiation into Foxp3-expressing Tregs occurs. The dependence of this increase on IL-10 and TGF-β_1 would suggest that it occurred in the tissues local to EtxB treatment or in the spleen and not at the site of activation, the draining lymph node of the OVA/CFA challenge (the inguinal lymph node in these studies). Although some changes in IL-10 and TGF-β_1 were observed in the inguinal lymph node following treatment (data not shown), these were much less pronounced than in other tissues and were not assessed following immunization with OVA/CFA, the addition of which would have presumably overwhelmingly biased the tissue toward an inflammatory phenotype. As minimal quantities of OVA are likely to reach the lymphoid tissues beyond the local draining lymph node, it seems likely that following activation, OVA-peptide-specific $CD4^+$ T cells leave lymph nodes associated with the inflammatory site and enter the modulated regulatory cytokine-biased environments created by EtxB elsewhere in the body, where their subsequent differentiation is affected. The fact that EtxB is immunogenic may aid this process, as lymphoid tissues affected by EtxB would become sites of activation and are likely to attract recently activated cells.

This model of EtxB action helps explain why mucosal treatment with EtxB protects from distinct autoimmune diseases that differ in their site of pathology. EtxB treatment was sufficient to prevent CIA development, both prophylactically and during disease progression.[13] In both cases, activated CII-specific $CD4^+$ T cells could have migrated from the draining lymph nodes at the joints to EtxB-modulated tissues, where their differentiation would become altered. This is supported by the fact that CII-specific $CD4^+$ T-cell interferon-γ production but not proliferation was inhibited by EtxB treatment, suggesting that differentiation but not activation was altered by EtxB treatment.[13] In T1D, EtxB treatment alone was only effective at preventing disease devel-

opment at an age when inflammation of the islets was already established,[12] again implicating that activation occurs at the site of disease and that modulation only happens once these cells have become activated and have migrated to EtxB-modulated tissues.

Determining the mechanisms by which pathogens, and their products, induce Treg at mucosal sites is important for understanding disease pathogenesis. To what extent the pathway shown here for EtxB occurs in the normal pathogenic process of enteropathogenic *E. coli* infection is undetermined. Following dissociation of EtxA and EtxB within epithelial cells, EtxB is detectable on the basolateral membrane,[24] meaning that free EtxB may be released and possibly able to mediate these effects. Treg responses may benefit the pathogen; however, the host may also benefit by reducing immunopathology. Additionally, the acute induction of regulatory cytokines may themselves limit innate reactivity and consequent damage to the integrity of the mucosal surface. Interestingly, Etx and EtxB are known to induce IgA production;[34] this may also be linked to the effects seen here as it is also a TGF-β_1-mediated process.

The generation or expansion of Tregs with defined antigen specificities is currently an attractive therapeutic goal, and the fact that EtxB promotes the generation of Tregs that are specific for antigens that are driving inflammatory immune responses elsewhere in the body makes it of particular interest. Such a mechanism of action permits the modulation of disease-associated pathogenic responses in the absence of modulation of responses to antigens that are not actively triggering T-cell activation at the time of treatment. Importantly, EtxB is effective when the cognate antigen is administered in the presence of strong inflammatory stimuli, as treatment of human autoimmune disease would be in the context of on-going inflammation, and inducing tolerance during this may be problematic for other treatments.

METHODS

Reagents and antibodies. Recombinant EtxB and EtxB(G33D) were purified as previously reported.[20] The lipopolysaccharide content was routinely < 30 endotoxin units (EU) per mg. EtxB was labelled using an Alexa Flour 647 protein labeling kit (Invitrogen) as per the manufacturer's instructions.

Antibodies used for immunohistochemistry were anti-cholera toxin (polyclonal; Sigma, Poole, UK), anti-IL-10 (JES5-2AS; Invitrogen), and anti-TGF-β1 (polyclonal; Santa Cruz Biotechnology, Santa Cruz, CA). Purified rat IgG1 (A110-1; BD Biosciences, Oxford, UK) and rabbit normal IgG (Santa Cruz Biotechnology) were used as isotype controls. Antibodies used for flow cytometry were anti-mouse CD16/CD32 (2.4G2), fluorescein isothiocyanate-conjugated anti-mouse CD4 (H129.19), phycoerythrin-conjugated anti-mouse CD25 (PC61), CD11b (M1/70), CD11c (HL3), B220 (RA3-6B2), and CD8a (53-6.7) (all from BD Biosciences), allophycocyanin-conjugated anti-mouse Foxp3 (FJK-16s) (eBioscience, San Diego, CA), and Tricolor-conjugated anti-DO11.10 TCR (KJ1-26) (Invitrogen). Anti-interferon-γ (XmG1.2), blocking anti-IL-10R (1B1.2),[35] and anti-pan TGF-β (1D11)[36] were purified from supernatants using a Protein G column and Aktaprime (GE Healthcare, Buckinghamshire, UK). Normal rat and mouse IgG (both from Invitrogen) were dialyzed in sterile PBS for 48 h.

Experimental animals. Male DBA/1 and female BALB/c and DO11.10 mice (bred at University of Bristol) were housed under barrier-maintained conditions and cared for in accordance with the Animals (Scientific Procedure) Act 1986 of the United Kingdom. Intranasal administration of 20 µl of 1 mg ml^{-1} EtxB, EtxB(G33D), Alexa 647-labeled EtxB, or PBS took place under anesthetic on four consecutive days. Antigenic challenges were performed on day 1 post-treatment by a single subcutaneous base of tail injection of OVA (Sigma) (in PBS) in an equal volume of CFA (Sigma). Adoptive transfer of DO11.10 CD4$^+$ T cells (5×10^6) was achieved by intravenous injection in the tail vein. Blocking antibodies were injected intraperitoneally on the third day of treatment.

Cell preparation, enrichment, and purification. Single-cell suspensions were prepared from CLNs and spleen by standard mechanical disruption or collagenase digestion where stated. Red blood cells were removed by standard ammonium chloride lysis. NALT cells were prepared using a previously described method.[37] For mRNA extraction and phenotyping of Alexa 647$^+$ cells, samples from separate mice were pooled before preparation of mRNA/single-cell suspensions. Peripheral blood was obtained by cardiac puncture and peripheral blood mononuclear cells isolated using Histopaque 1083 (Sigma).

CD4$^+$, B220$^+$, and CD11b$^+$ cells were purified using magnetic-activated cell sorting CD4$^+$, B220$^+$, and CD11b$^+$ microbeads (Miltenyi Biotech, Bisley, UK) according to the manufacturer's instructions and were >95% pure. CD4$^+$CD25$^+$ and CD4$^+$CD25$^-$ T subsets were sorted using a FACSVantage (BD Biosciences) and were >98% pure. Nylon wool-enriched splenic lymphocytes were routinely >65% CD4$^+$.

Immunohistochemistry and analysis. CLNs and spleen samples were fixed and embedded in low-temperature wax as previously described.[38] NALT were formalin fixed and decalcified in Kristensen's decalcification solution (20% formic acid (v/v) (VWR), 0.63 M formic acid (sodium salt) (Sigma)) for 7 days at 4 °C prior to embedding. Immunohistochemical staining using the aforementioned antibodies was performed on 6 µm sections as previously described.[38,39]

A quantitative analysis of each tissue was performed to estimate the area of positive staining using KS300 AxioVision from Zeiss (Image Associates, Bicester, UK). For CLNs and spleen, the total area and the area of positive staining was measured in three fields of view (FoV) per section (×3 sections, 9 FoV total), from which the mean percentage positive stained area was calculated. For NALT, one FoV was analyzed per section (×6 sections, 6 FoV total).

Flow cytometry. Fc receptors were blocked with anti-CD16/32, followed by incubation with appropriate combinations of antibodies for 30 min at 4 °C. Intracellular Foxp3 staining was achieved using a Foxp3 staining kit (eBioscience) as per the manufacturer's instructions. At least 1×10^5 (Foxp3 expression) or 1×10^6 (phenotyping of Alexa 647$^+$ cells; detection of KJ1-26$^+$ cells) events were collected for each sample using a FACSCalibur flow cytometer (BD Biosciences) and were analyzed using WinMDI 2.8 (J. Trotter, Scripps Research Institute).

Reverse transcriptase-PCR. Total RNA was extracted using Tri-reagent (Sigma) according to the manufacturer's instructions. First-strand complementary DNA was synthesized using superscript complementary DNA synthesis system (Invitrogen). Reverse transcriptase-PCR was performed using primers specific for murine IL-10,[40] TGF-β,[41] Foxp3,[6] and HPRT[6] (Invitrogen) as previously described using a Peltier thermal cycler (MJ Research, Waltham, MA) and 1.5 U BioTaq DNA polymerase (Bioline, London, UK). Densitometry was performed on gel images using ImageJ (US National Institutes of Health, Bethesda, MD).

Statistical analysis. Statistical analyses were performed using Graphpad Prism 4 (Graphpad Software, San Diego, CA). Results are expressed as mean±s.e.m. A one-way ANOVA with Tukey's multiple comparisons *post hoc* test was performed on immunohistochemical data. Other data were analyzed using Student's *t-test*. Significant differences shown in figures refer to differences with the untreated control.

SUPPLEMENTARY MATERIAL is linked to the online version of the paper at http://www.nature.com/mi

ACKNOWLEDGMENTS

This work was supported by grants from the Medical Research Council (UK) and the Arthritis Research Campaign. We thank R. Williams and B.B. Daniels for preparing EtxB, and A. Herman, D.J. Morgan, and J. Baker for technical advice and assistance.

DISCLOSURE

N.A.W. is a shareholder in Trident Pharmaceuticals, which holds patent rights to the use of EtxB as a treatment for inflammatory disease. The other authors declared no conflict of interest.

REFERENCES

1. Sakaguchi, S., Sakaguchi, N., Asano, M., Itoh, M. & Toda, M. Immunologic self-tolerance maintained by activated T cells expressing IL-2 receptor alpha-chains (CD25). Breakdown of a single mechanism of self-tolerance causes various autoimmune diseases. *J. Immunol.* **155,** 1151–1164 (1995).
2. Asano, M., Toda, M., Sakaguchi, N. & Sakaguchi, S. Autoimmune disease as a consequence of developmental abnormality of a T cell subpopulation. *J. Exp. Med.* **184,** 387–396 (1996).
3. Groux, H. *et al.* A CD4+ T-cell subset inhibits antigen-specific T-cell responses and prevents colitis. *Nature* **389,** 737–742 (1997).
4. Chen, Y., Kuchroo, V.K., Inobe, J., Hafler, D.A. & Weiner, H.L. Regulatory T cell clones induced by oral tolerance: suppression of autoimmune encephalomyelitis. *Science* **265,** 1237–1240 (1994).
5. Khattri, R., Cox, T., Yasayko, S.A. & Ramsdell, F. An essential role for Scurfin in CD4+CD25+ T regulatory cells. *Nat. Immunol.* **4,** 337–342 (2003).
6. Hori, S., Nomura, T. & Sakaguchi, S. Control of regulatory T cell development by the transcription factor Foxp3. *Science* **299,** 1057–1061 (2003).
7. Fontenot, J.D., Rasmussen, J.P., Williams, L.M., Dooley, J.L., Farr, A.G. & Rudensky, A.Y. Regulatory T cell lineage specification by the forkhead transcription factor foxp3. *Immunity* **22,** 329–341 (2005).
8. Fantini, M.C., Becker, C., Monteleone, G., Pallone, F., Galle, P.R. & Neurath, M.F. Cutting edge: TGF-beta induces a regulatory phenotype in CD4+CD25- T cells through Foxp3 induction and down-regulation of Smad7. *J. Immunol.* **172,** 5149–5153 (2004).
9. Rao, P.E., Petrone, A.L. & Ponath, P.D. Differentiation and expansion of T cells with regulatory function from human peripheral lymphocytes by stimulation in the presence of TGF-{beta}. *J. Immunol.* **174,** 1446–1455 (2005).
10. Chen, W. *et al.* Conversion of peripheral CD4+CD25- naive T cells to CD4+CD25+ regulatory T cells by TGF-beta induction of transcription factor Foxp3. *J. Exp. Med.* **198,** 1875–1886 (2003).
11. Belkaid, Y. & Rouse, B.T. Natural regulatory T cells in infectious disease. *Nat. Immunol.* **6,** 353–360 (2005).
12. Ola, T.O. & Williams, N.A. Protection of non-obese diabetic mice from autoimmune diabetes by Escherichia coli heat-labile enterotoxin B subunit. *Immunology* **117,** 262–270 (2006).
13. Luross, J.A., Heaton, T., Hirst, T.R., Day, M.J. & Williams, N.A. Escherichia coli heat-labile enterotoxin B subunit prevents autoimmune arthritis through induction of regulatory CD4+ T cells. *Arthritis Rheum.* **46,** 1671–1682 (2002).
14. Spangler, B.D. Structure and function of cholera toxin and the related Escherichia coli heat-labile enterotoxin. *Microbiol. Rev.* **56,** 622–647 (1992).
15. Sixma, T.K., Stein, P.E., Hol, W.G. & Read, R.J. Comparison of the B-pentamers of heat-labile enterotoxin and verotoxin-1: two structures with remarkable similarity and dissimilarity. *Biochemistry* **32,** 191–198 (1993).
16. Cassel, D. & Pfeuffer, T. Mechanism of cholera toxin action: covalent modification of the guanyl nucleotide-binding protein of the adenylate cyclase system. *Proc. Natl. Acad. Sci. USA* **75,** 2669–2673 (1978).
17. Nashar, T.O., Hirst, T.R. & Williams, N.A. Modulation of B-cell activation by the B subunit of Escherichia coli enterotoxin: receptor interaction up-regulates MHC class II, B7, CD40, CD25 and ICAM-1. *Immunology* **91,** 572–578 (1997).
18. Nashar, T.O., Webb, H.M., Eaglestone, S., Williams, N.A. & Hirst, T.R. Potent immunogenicity of the B subunits of Escherichia coli heat-labile enterotoxin: receptor binding is essential and induces differential modulation of lymphocyte subsets. *Proc. Natl. Acad. Sci. USA* **93,** 226–230 (1996).
19. Truitt, R.L., Hanke, C., Radke, J., Mueller, R. & Barbieri, J.T. Glycosphingolipids as novel targets for T-cell suppression by the B subunit of recombinant heat-labile enterotoxin. *Infect. Immun.* **66,** 1299–1308 (1998).
20. Turcanu, V., Hirst, T.R. & Williams, N.A. Modulation of human monocytes by Escherichia coli heat-labile enterotoxin B-subunit; altered cytokine production and its functional consequences. *Immunology* **106,** 316–325 (2002).
21. Peng, Y., Laouar, Y., Li, M.O., Green, E.A. & Flavell, R.A. TGF-beta regulates in vivo expansion of Foxp3-expressing CD4+CD25+ regulatory T cells responsible for protection against diabetes. *Proc. Natl. Acad. Sci. USA* **101,** 4572–4577 (2004).
22. Goudy, K.S. *et al.* Systemic overexpression of IL-10 induces CD4+CD25+ cell populations in vivo and ameliorates type 1 diabetes in nonobese diabetic mice in a dose-dependent fashion. *J. Immunol.* **171,** 2270–2278 (2003).
23. Griffiths, S.L., Finkelstein, R.A. & Critchley, D.R. Characterization of the receptor for cholera toxin and Escherichia coli heat-labile toxin in rabbit intestinal brush borders. *Biochem. J.* **238,** 313–322 (1986).
24. Lindner, J., Geczy, A.F. & Russell-Jones, G.J. Identification of the site of uptake of the E. coli heat-labile enterotoxin, LTB. *Scand. J. Immunol.* **40,** 564–572 (1994).
25. Lencer, W.I., Moe, S., Rufo, P.A. & Madara, J.L. Transcytosis of cholera toxin subunits across model human intestinal epithelia. *Proc. Natl. Acad. Sci. USA* **92,** 10094–10098 (1995).
26. Richards, C.M., Aman, A.T., Hirst, T.R., Hill, T.J. & Williams, N.A. Protective mucosal immunity to ocular herpes simplex virus type 1 infection in mice by using Escherichia coli heat-labile enterotoxin B subunit as an adjuvant. *J. Virol.* **75,** 1664–1671 (2001).
27. Liu, G., Wu, C., Wu, Y. & Zhao, Y. Phagocytosis of apoptotic cells and immune regulation. *Scand. J. Immunol.* **64,** 1–9 (2006).
28. Pillai, V., Ortega, S.B., Wang, C.K. & Karandikar, N.J. Transient regulatory T-cells: a state attained by all activated human T-cells. *Clin. Immunol.* **123,** 18–29 (2007).
29. Sun, J.B., Cuburu, N., Blomquist, M., Li, B.L., Czerkinsky, C. & Holmgren, J. Sublingual tolerance induction with antigen conjugated to cholera toxin B subunit induces Foxp3+CD25+CD4+ regulatory T cells and suppresses delayed-type hypersensitivity reactions. *Scand. J. Immunol.* **64,** 251–259 (2006).
30. Sun, J.B., Raghavan, S., Sjoling, A., Lundin, S. & Holmgren, J. Oral tolerance induction with antigen conjugated to cholera toxin B subunit generates both Foxp3+CD25+ and Foxp3-CD25- CD4+ regulatory T cells. *J. Immunol.* **177,** 7634–7644 (2006).
31. Apostolaki, M. & Williams, N.A. Nasal delivery of antigen with the B subunit of Escherichia coli heat-labile enterotoxin augments antigen-specific T-cell clonal expansion and differentiation. *Infect. Immun.* **72,** 4072–4080 (2004).
32. Liu, H., Hu, B., Xu, D. & Liew, F.Y. CD4+CD25+ regulatory T cells cure murine colitis: the role of IL-10, TGF-beta, and CTLA4. *J. Immunol.* **171,** 5012–5017 (2003).
33. Cottrez, F. & Groux, H. Regulation of TGF-beta response during T cell activation is modulated by IL-10. *J. Immunol.* **167,** 773–778 (2001).
34. Nakagawa, I., Takahashi, I., Kiyono, H., McGhee, J.R. & Hamada, S. Oral immunization with the B subunit of the heat-labile enterotoxin of Escherichia coli induces early Th1 and late Th2 cytokine expression in Peyer's patches. *J. Infect. Dis.* **173,** 1428–1436 (1996).
35. O'Farrell, A.M., Liu, Y., Moore, K.W. & Mui, A.L. IL-10 inhibits macrophage activation and proliferation by distinct signaling mechanisms: evidence for Stat3-dependent and -independent pathways. *EMBO J.* **17,** 1006–1018 (1998).
36. Dasch, J.R., Pace, D.R., Waegell, W., Inenaga, D. & Ellingsworth, L. Monoclonal antibodies recognizing transforming growth factor-beta. Bioactivity neutralization and transforming growth factor beta 2 affinity purification. *J. Immunol.* **142,** 1536–1541 (1989).
37. Asanuma, H. *et al.* Isolation and characterization of mouse nasal-associated lymphoid tissue. *J. Immunol. Methods* **202,** 123–131 (1997).
38. Whiteland, J.L., Nicholls, S.M., Shimeld, C., Easty, D.L., Williams, N.A. & Hill, T.J. Immunohistochemical detection of T-cell subsets and other leukocytes in paraffin-embedded rat and mouse tissues with monoclonal antibodies. *J. Histochem. Cytochem.* **43,** 313–320 (1995).
39. Whiteland, J.L., Shimeld, C., Nicholls, S.M., Easty, D.L., Williams, N.A. & Hill, T.J. Immunohistochemical detection of cytokines in paraffin-embedded mouse tissues. *J. Immunol. Methods* **210,** 103–108 (1997).
40. Yang, J., Lindsberg, P.J., Hukkanen, V., Seljelid, R., Gahmberg, C.G. & Meri, S. Differential expression of cytokines (IL-2, IFN-gamma, IL-10) and adhesion molecules (VCAM-1, LFA-1, CD44) between spleen and lymph nodes associates with remission in chronic relapsing experimental autoimmune encephalomyelitis. *Scand. J. Immunol.* **56,** 286–293 (2002).
41. Kawakami, K., Tohyama, M., Qifeng, X. & Saito, A. Expression of cytokines and inducible nitric oxide synthase mRNA in the lungs of mice infected with Cryptococcus neoformans: effects of interleukin-12. *Infect. Immun.* **65,** 1307–1312 (1997).